FZL, an FZO-like protein in plants, is a determinant of thylakoid and chloroplast morphology

Hongbo Gao*†‡, Tammy L. Sage§, and Katherine W. Osteryoung*¶

*Department of Plant Biology and †Genetics Graduate Program, Michigan State University, East Lansing, MI 48824; and §Department of Botany, University of Toronto, 25 Willcocks Street, Toronto, ON, Canada M5S 3B2

Edited by Roland Douce, University of Grenoble, Grenoble, France, and approved March 8, 2006 (received for review August 21, 2005)

FZO is a dynamin-related membrane-remodeling protein that mediates fusion between mitochondrial outer membranes in animals and fungi. We identified a single FZO-like protein in *Arabidopsis*, FZL, a new plant-specific member of the dynamin superfamily. FZL is targeted to chloroplasts and associated with thylakoid and envelope membranes as punctate structures. *fzl* knockout mutants have abnormalities in chloroplast and thylakoid morphology, including disorganized grana stacks and alterations in the relative proportions of grana and stroma thylakoids. Overexpression of FZL-GFP also conferred defects in thylakoid organization. Mutation of a conserved residue in the predicted FZL GTPase domain abolished both the punctate localization pattern and ability of FZL-GFP to complement the *fzl* mutant phenotype. FZL defines a new protein class within the dynamin superfamily of membrane-remodeling GTPases that regulates organization of the thylakoid network in plants. Notably, FZL levels do not affect mitochondrial morphology or ultrastructure, suggesting that mitochondrial morphology in plants is regulated by an FZO-independent mechanism.

dynamin superfamily | membrane dynamics | membrane remodeling | mitochondrial fusion | plastid

Mitochondria fuse frequently in eukaryotic cells, and the balance between mitochondrial fusion and fission determines the steady-state morphology of the organelle (1–3). Mutations in FZO, a member of the dynamin superfamily of membrane-remodeling proteins (1–5), block mitochondrial fusion, tipping the balance toward fission and causing mitochondria to fragment and lose DNA (6–9). Overexpression of FZO tips the balance toward fusion, inducing the formation of mitochondrial networks (10, 11). Thus, FZO is a key regulator of mitochondrial morphology in fungi and animals. FZO is localized in the outer mitochondrial membrane. It possesses a GTPase domain near its N terminus followed by two coiled-coil domains flanking a pair of transmembrane (TM) helices separated by a short loop (Fig. 1*A*). The GTPase and coiled-coil domains face the cytosol whereas the loop protrudes into the intermembrane space (1, 2, 12, 13). Intermolecular interactions between the coiled-coil domains of FZO are thought to mediate tethering between apposing outer mitochondrial membranes at an early step in the fusion pathway (2, 4, 9, 11, 14).

Chloroplasts in plant cells are also surrounded by two membranes. In addition, they contain an internal system of interconnected membranes, the thylakoids, that carry out the light reactions of photosynthesis. Lamellae comprising the thylakoid network are arranged into stacked and unstacked regions called grana and stroma thylakoids, respectively, that are differentially enriched in photosystem I and II complexes (15–17). This morphological and biochemical heterogeneity presumably increases the efficiency of photosynthesis. Although extensive, the thylakoid network in an individual chloroplast is thought to comprise a single lumenal compartment (17). Thylakoids are posited to arise from the inner envelope via a vesicle transport system (18–21), implicating membrane-trafficking processes in the organelle in maintenance of thylakoid morphology. Beyond this, however, the mechanisms governing the formation, spatial organization, and morphology of the thylakoid membranes are not understood.

Here we report the identification of an FZO-like protein in *Arabidopsis*, FZL, which is similar in both sequence and domain arrangement to mitochondrial FZO but is predicted to be targeted to chloroplasts. We show that FZL is indeed chloroplastic and is distributed between the thylakoid and envelope membranes. *fzl* mutants have abnormalities in the morphology and distribution of grana and stroma thylakoids consistent with a role in regulating thylakoid organization. Mutation of a conserved residue in the GTPase domain abolishes FZL function. An FZL-GFP fusion protein expressed in *Arabidopsis* could not be detected in mitochondria, nor did *fzl* mutants exhibit abnormalities in mitochondrial morphology. FZL thus defines a new plant-specific member of the dynamin superfamily of membrane-remodeling GTPases with a unique role in the determination of thylakoid and chloroplast morphology. Because FZL is the only FZO-like protein in *Arabidopsis*, these findings also raise the question of how mitochondrial morphology in plant cells is regulated.

Results

FZL Is an FZO-Like Protein in Plants. FZL (At1g03160) was identified by a BLAST search of the *Arabidopsis* protein database (www.arabidopsis.org/Blast) using *Drosophila* FZO as a query sequence. The *FZL* cDNA was amplified from *Arabidopsis* by RT-PCR and sequenced. The results showed that the annotated FZL amino acid sequence lacked 270 residues at the C terminus. A BLAST search of the NCBI database (www.ncbi.nlm.nih.gov/blast) confirmed that FZL shares similarity with FZO-related mitochondrial fusion proteins. *FZL* encodes a protein of 912 aa (Fig. 1*A*) and is conserved in many photosynthetic eukaryotes, including rice and *Chlamydomonas* (data not shown). FZL is most similar to FZO in its putative GTPase domain (Fig. 1*B*). The FZL sequence also predicts two TM domains separated by a short linker and two coiled-coil domains flanking the predicted TM domains. This domain arrangement is very similar to that of FZO (2) (Fig. 1*A*). Interestingly, FZL was predicted by TARGETP (22) (www.cbs.dtu.dk/services/TargetP) to have a chloroplast transit peptide (score, 0.871; reliability class, 2) comprising the first 54 amino acid residues at the N terminus (Fig. 1*A*), suggesting that FZL may be targeted to the chloroplast *in vivo*.

Phylogenetic analysis was performed to investigate the relationship between FZL and other members of the dynamin superfamily (Fig. 1*C*). Because the sequences are divergent, only the GTPase domains were aligned for the analysis. FZL and its homolog in rice formed a branch near the clade bearing FZO (Fig. 1*C*). These data suggest that *FZL* and *FZO*, or at least their GTPase domains, may

Conflict of interest statement: No conflicts declared.

This paper was submitted directly (Track II) to the PNAS office.

Abbreviation: TM, transmembrane.

Data deposition: The cDNA sequence reported in this paper has been deposited in the GenBank database (accession no. DQ462573).

‡Present address: Department of Energy Plant Research Laboratory, Michigan State University, East Lansing, MI 48824.

¶To whom correspondence should be addressed at: Department of Plant Biology, 166 Plant Biology Building, Michigan State University, East Lansing, MI 48824. E-mail: osteryou@msu.edu.

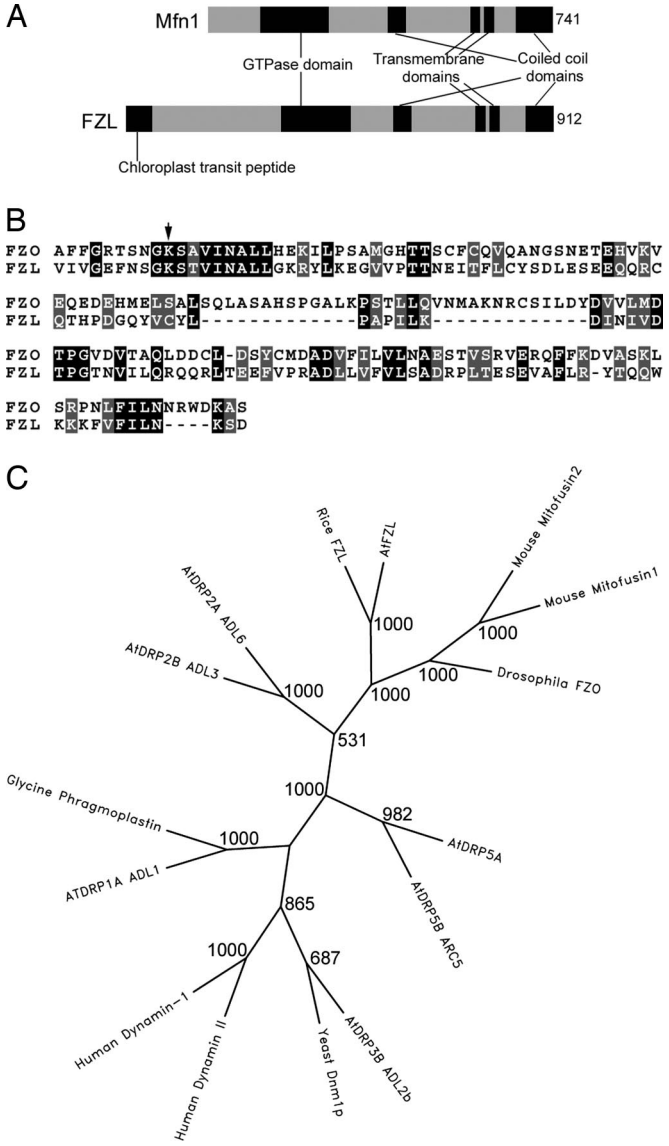

Fig. 1. FZL is an FZO-like protein in plants. (*A*) Domain structure of the mouse FZO ortholog Mitofusin 1 (Mfn1) and predicted domains of *Arabidopsis* FZL. (*B*) Alignment of the FZL and *Drosophila melanogaster* FZO GTPase domains. Black, identical residues; gray, similar residues. Dashes indicate gaps. An arrow indicates a mutated residue in *FZL(K362M)-GFP*. (*C*) Unrooted phylogenetic tree of dynamin superfamily proteins based on alignment of GTPase domains. Bootstrap values from neighbor-joining analysis are shown at nodes with >50% bootstrap support. ''At'' denotes *A. thaliana*. GenBank accession numbers for proteins shown are as follows: FZL, NM_100198; human Dynamin 1, NP_004399; human Dynamin II, NP_004936; yeast Dnm1p, NP_013100; AtDRP3B, NP_565362; AtDRP1A, NP_851120; glycine phragmoplastin, AAB05992; AtDRP2A, AAF22291; AtDRP2B, NP_176170; AtDRP5A, NP_175722; AtDRP5B, AY212885; *Drosophila* FZO, AAF56110; rice FZL, XP_475185; mouse Mitofusin 1, AAH56641; mouse Mitofusin 2, AAM88577.

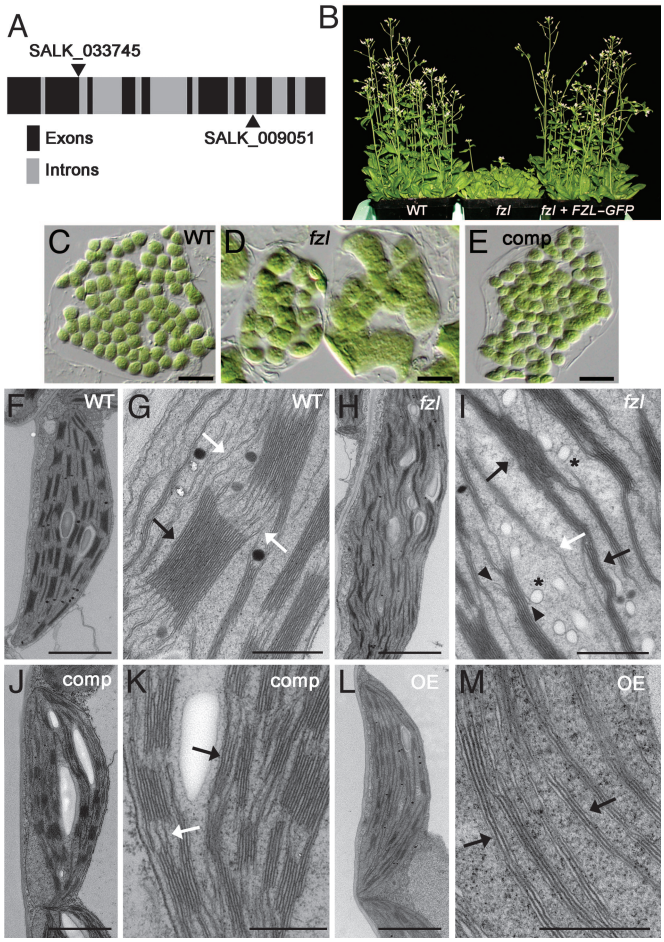

Fig. 2. *FZL* affects chloroplast morphology, plant growth, and thylakoid ultrastructure. (*A*) Gene structure of *FZL*. Black, exons; gray, introns. T-DNA insertion sites in the two *fzl* Salk mutants are indicated by arrowheads. (*B*) *fzl* mutants look pale and flower later than WT. (*Left*) WT. (*Center*) *fzl* mutant. (*Right*) *fzl* mutant complemented by *FZL-GFP*. (*C–E*) Chloroplast morphology and division phenotypes in mesophyll cells from 4-week-old expanded leaves. (*C*) Single cell from WT. (*D*) Two cells from an *fzl* mutant. (*E*) Single cell from an *fzl* mutant complemented by *FZL-GFP*. (*F–M*) Ultrastructure of chloroplasts from plants expressing different levels of FZL-GFP. (*F* and *G*) WT. (*H* and *I*) *fzl*. (*J* and *K*) *fzl* mutant complemented by *FZL-GFP* (comp). (*L* and *M*) *fzl* mutant expressing FZL-GFP above levels required to complement *fzl* (OE). Black and white arrows mark grana and stroma thylakoids, respectively. Arrowheads denote inflated lamellae of unevenly stacked *fzl* grana. *, vesicle-like traits in *fzl*. (Scale bars: 10 μm in *C–E*; 2 μm in *F*, *H*, *J*, and *L*; 500 nm in *G*, *I*, *K*, and *M*.)

have arisen from an ancestral gene in the common ancestor of plants and animals.

Loss of *FZL* Function Alters Chloroplast and Thylakoid Morphology. We obtained two *FZL* T-DNA insertional mutants (23) (Fig. 2*A*) from the *Arabidopsis* Biological Resource Center (Columbus, OH). The insertion in Salk_033745 is in the region encoding the GTPase domain. Salk_009051 has two tandem insertions, one in an intron between the exons encoding the second TM domain and a second in the 3′ UTR (data not shown). Both *fzl* alleles conferred the same phenotypes. The leaves were visibly pale, and flowering was delayed by 5–7 days compared with the *Col-0* WT (Fig. 2*B*). Mature mesophyll cells in the *fzl* knockout lines contained fewer, larger chloroplasts than in WT, and these were heterogeneous in size (Fig. 2 *C* and *D*). This phenotype was more pronounced in older than in younger leaves (data not shown).

Mesophyll cell chloroplasts in WT and *fzl* plants also differed ultrastructurally. In WT, the lamellae comprising the grana thylakoids were similar in length and evenly stacked, and stroma thylakoids spanning the grana were frequent (Fig. 2 *F* and *G*). In *fzl* mutants, grana lamellae were less uniform in length and stacked in a staggered fashion, giving rise to a disorganized thylakoid array (Fig. 2 *H* and *I*). Stroma thylakoids appeared less abundant than in WT. Although the mean number of lamellae/granum did not differ significantly between WT and *fzl*, grana were longer in *fzl* than in WT (Fig. 2 *F–I*, Table 1, and Fig. 6, which is published as supporting information on the PNAS web site). In contrast, stroma thylakoids

Table 1. Quantitative analysis of thylakoid morphological traits

Genotype	No. of lamellae per granum	Grana thylakoid length,* nm	Stroma thylakoid length,* nm	Stroma thylakoids/total thylakoids
Col-0 (WT)	8.9 ± 1.7[a]	702 ± 54[a]	456 ± 104[a]	0.09 ± 0.02[a]
fzl	7.6 ± 0.9[a]	1092 ± 99[b]	470 ± 100[a]	0.05 ± 0.01[b]
fzl complemented by *FZL-GFP*	6.6 ± 0.8[a]	472 ± 39[c]	267 ± 38[b]	0.11 ± 0.03[a]
fzl overexpressing *FZL-GFP*	4.4 ± 0.7[b]	1428 ± 261[b]	188 ± 161[b]	0.03 ± 0.02[b]

Values for 95% confidence interval in a single column with the same superscript letters a, b, or c do not differ significantly; values with different superscript letters differ significantly.
*See Fig. 6 for an explanation of length measurements.

in *fzl* were similar in length to those in WT but constituted a smaller proportion of the total thylakoid network (Table 1). Intriguingly, some grana lamellae were inflated at their margins, and vesicle-like structures were frequently observed (Fig. 2*I*).

To confirm that the mutant phenotypes resulted from disruption of *FZL*, the *FZL* coding region fused to *GFP* at its 3′ end was expressed in *fzl* mutant plants under control of the *FZL* promoter. The mutant phenotypes (including the pale leaves, delayed flowering, and chloroplast morphology and ultrastructure defects) were largely rescued by the transgene (Fig. 2 *B*, *E*, *J*, and *K*). However, the mean lengths of grana and stroma thylakoids were lower in the complementation lines than in WT, although their relative proportions were restored (Table 1). These results reveal a role for FZL in regulating thylakoid organization and chloroplast morphology. The complementation results also demonstrated that the GFP fusion protein encoded by the transgene was functional.

FZL Is Localized to Chloroplasts. To determine whether the predicted transit peptide of FZL (tpFZL) mediates chloroplast targeting, the coding sequence from the 3rd to the 67th amino acid residue was fused to GFP. The resulting transgene, *35S-tpFZL-GFP*, was expressed in WT *Arabidopsis* plants on a CaMV 35S promoter. In mesophyll cells of transgenic plants, the GFP signal was coincident with chlorophyll autofluorescence, indicating its association with chloroplasts (Fig. 3 *A–C*). In plants expressing a control GFP construct lacking tpFZL, the GFP remained in the cytosol (Fig. 3 *D–F*). Only the chlorophyll autofluorescence could be detected in WT plants (Fig. 3 *G–I*). These results confirmed the prediction of TARGETP that FZL has a functional chloroplast transit peptide.

To assess the *in vivo* localization of FZL, we took advantage of *fzl* plants that had been complemented by the functional *FZL-GFP* transgene (Fig. 2 *B*, *E*, *J*, and *K*). Expression levels varied in different transgenic lines as indicated by visibly detectable differences in the GFP signal (Fig. 3 *K* and *L*) and the amount of GFP-tagged fusion protein on immunoblots (Fig. 3*O*). In all cases, however, FZL-GFP exhibited a punctate pattern of localization (Fig. 3 *K–N*). At lower levels of expression (Fig. 3 *K* and *O*, lanes 3 and 4), FZL-GFP puncta were most evident at the chloroplast periphery, although very faint puncta could be detected in the organelle interior. At higher levels (Fig. 3 *L* and *O*, lanes 7 and 8), small puncta were clearly visible throughout the chloroplast (Fig. 3 *M* and *N*). The association of FZL-GFP with the chloroplast is consistent with the presence of a chloroplast transit peptide (Fig. 3 *A–C*). On rare occasions, FZL-GFP puncta that appeared separated from the chloroplasts could also be observed (Fig. 7, which is published as supporting information on the PNAS web site).

FZL-GFP Is a Membrane Protein Associated with both the Thylakoid and Envelope. We investigated the subplastidic localization of FZL-GFP by carrying out a series of protease protection and fractionation assays using chloroplasts isolated from the transgenic *fzl* plants complemented by *FZL-GFP*. In the first set of experiments we treated intact chloroplasts with the protease thermolysin, which cannot penetrate the outer envelope, or trypsin, which penetrates the outer but not the inner envelope (24), and we used immunoblotting with anti-GFP antibodies to determine the susceptibility of FZL-GFP to proteolysis. As a stromal marker we used Tic110, an inner-envelope protein facing the stroma (25). As an intermembrane space marker we used a C-terminal GFP fusion to ARC6, an inner-envelope protein whose C terminus faces the intermembrane space (26). The marker proteins behaved as ex-

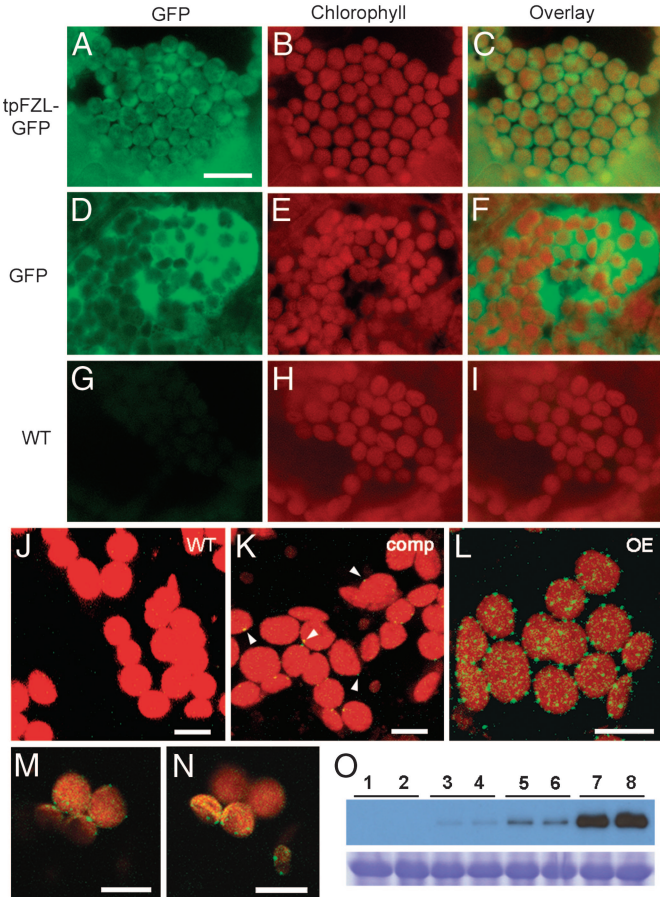

Fig. 3. FZL-GFP localizes to chloroplasts in a punctate pattern. (*A–I*) FZL has a chloroplast transit peptide. Single cells imaged by fluorescence microscopy are shown. (*A–C*) Plant transformed by *35S-tpFZL-GFP*. (*D–F*) Plant transformed by *35S-GFP*. (*G–I*) WT. (*J–O*) FZL-GFP localizes to punctate structures. Extended-focus (*J–L*) or single-section (image depth, 0.5 μm) (*M* and *N*) confocal images are shown. (*K*) *fzl* complemented by FZL-GFP. Arrowheads show GFP signals at edges of chloroplasts. (*L*) *fzl* with a high level of FZL-GFP. (*O Upper*) FZL-GFP detected by immunoblotting in *fzl* transgenic lines expressing different FZL-GFP levels. (*O Lower*) Equal loading is shown by Coomassie staining. Lanes 1 and 2, *fzl*; lanes 3 and 4, *fzl* partially complemented by FZL-GFP; lanes 5 and 6, *fzl* fully complemented by FZL-GFP; lanes 7 and 8, *fzl* plants with high FZL-GFP levels. (Scale bars: 10 μm in *A–I* and 5 μm in *J–N*.)

PLANT BIOLOGY

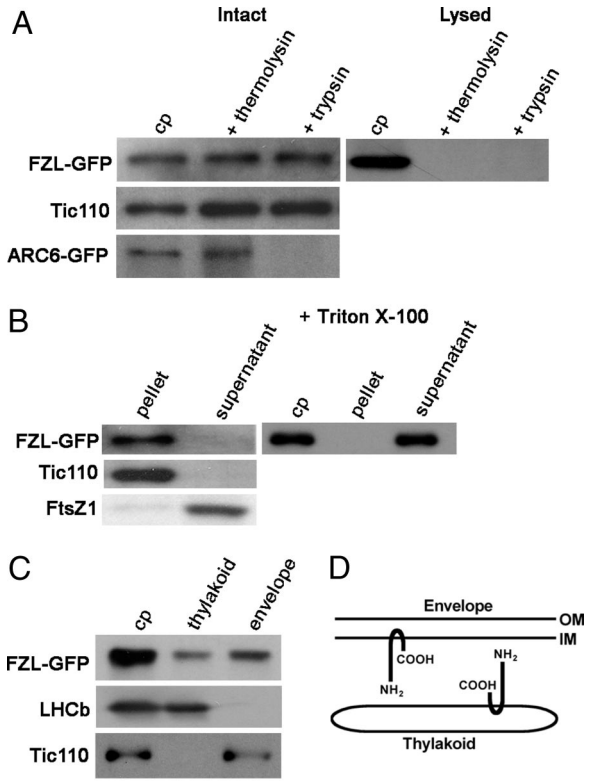

Fig. 4. FZL is localized in envelope and thylakoid membranes. (*A*) Isolated intact (*Left*) or lysed (*Right*) chloroplasts were incubated with thermolysin and trypsin. (*B Left*) Isolated chloroplasts were lysed osmotically and separated into pellet and supernatant fractions. (*B Right*) FZL-GFP is solubilized by 1% Triton X-100. (*C*) Isolated chloroplasts were lysed osmotically and separated into thylakoid and envelope fractions. In *A–C*, crude proteins representing approximately equivalent proportions of the chloroplast from each fraction were analyzed by SDS/PAGE and immunoblotting with antibodies against GFP, the inner-envelope protein Tic110, the soluble stromal protein FtsZ1, or the thylakoid membrane protein LHCb. cp, chloroplast. (*D*) Predicted topology of FZL in the envelope and thylakoid membranes. OM, outer-envelope membrane; IM, inner-envelope membrane.

pected (Fig. 4*A*); ARC6-GFP was susceptible to trypsin but not thermolysin, whereas Tic110 was protected from both proteases. Like Tic110, FZL-GFP was fully protected from both proteases (Fig. 4*A Left*). If chloroplasts were lysed before protease treatment, however, FZL-GFP was degraded (Fig. 4*A Right*), indicating that protection from thermolysin and trypsin was due to inaccessibility of the proteases to FZL-GFP and not to protein folding. These results show that FZL-GFP is targeted to the stromal side of the chloroplast envelope.

To determine whether FZL is a membrane protein, the isolated chloroplasts were lysed in hypotonic solution and separated into pellet and soluble fractions by centrifugation. FZL-GFP and the inner-envelope marker Tic110 (25) were both found in the pellet fraction by immunoblotting whereas the soluble stromal marker protein FtsZ1 (24) was detected mainly in the soluble fraction (Fig. 4*B Left*). FZL-GFP could be solubilized by treatment of the pellet fraction with Triton X-100 (Fig. 4*B Right*). These data confirm that FZL is a membrane protein as predicted by sequence analysis (Fig. 1*A*).

To determine which chloroplast membrane fraction contained FZL-GFP, membranes from hypotonically lysed chloroplasts were fractionated into thylakoid and envelope fractions (27). Immunoblot analysis indicated that FZL-GFP was present in both fractions (Fig. 4*C*). As controls, Tic110 and the thylakoid marker LHCb were detected only in the envelope and thylakoid fractions, respectively. Together, the membrane fractionation and protease protection experiments provide evidence that FZL is a chloroplast membrane protein distributed between the envelope and thylakoid membranes. Furthermore, because FZL-GFP is protected from trypsin as well as thermolysin (Fig. 4*A*), the results indicate that the fraction of FZL associated with the envelope is in the inner-envelope membrane and that the bulk of the protein faces the stroma.

FZL-GFP Levels and the Number of GFP-Labeled Punctate Structures Are Correlated. We compared chloroplast morphology, thylakoid ultrastructure, and GFP labeling patterns in *fzl* plants expressing FZL-GFP at different levels. When FZL-GFP was expressed at a level that complemented the chloroplast morphology and ultrastructure phenotypes of *fzl* mutants (Figs. 2 *E*, *J*, and *K* and 3*O*, lanes 5 and 6), the GFP signal was detected primarily in a few punctate structures near the organelle periphery (Fig. 3*K*), although fractionation also showed FZL-GFP in the thylakoids (Fig. 4*C*). At lower FZL-GFP levels (Fig. 3*O*, lanes 3 and 4), partial rescue of both chloroplast morphology and ultrastructure phenotypes was observed, although GFP fluorescence was not readily detectable (data not shown). At higher levels (Fig. 3*O*, lanes 7 and 8) the chloroplast morphology defects were fully rescued (red autofluorescence in Fig. 3*L*), but the distribution between grana and stroma thylakoids was perturbed and very few completely unstacked lamellae were observed (Table 1 and Fig. 2 *L* and *M*). These overexpression lines had more GFP-labeled punctate structures at the chloroplast periphery and in the organelle interior (Fig. 3 *L–N*), were also slightly more pale than WT, and flowered a few days earlier (data not shown). Overall, the number and size of GFP-labeled punctate structures increased with increasing FZL-GFP expression level. Together with the abnormalities observed in the *fzl* mutants, these experiments indicate that the level of FZL influences the morphology and organization of thylakoids.

The GTPase Domain Is Important for FZL Function. Lysine 362 in the predicted GTPase domain of FZL (Fig. 1*B*, arrow) is conserved in the active sites of many GTPases (5, 28). Mutation of the equivalent residue in FZO has been shown to abolish its function (6, 13). To investigate the importance of the predicted GTPase domain for FZL function, we mutated lysine 362 in FZL-GFP to methionine to produce *FZL(K362M)-GFP* and expressed the transgene in *fzl* mutant and WT plants under control of the *FZL* promoter.

Immunoblotting showed that FZL(K362M)-GFP accumulated to levels comparable to those of FZL-GFP (Fig. 5*A*). However, FZL(K362M)-GFP failed to rescue the *fzl* chloroplast morphology defects at any level of expression (Fig. 5*B*). Furthermore, the mutant protein could not be detected in punctate structures in either the *fzl* or WT backgrounds (Fig. 5 *B* and *C*). These findings suggest that GTP binding and/or hydrolysis is required both for FZL function and for its punctate pattern of localization and that the punctate localization reflects an important property of FZL function.

FZL Does Not Influence Mitochondrial Morphology. In yeast and animals, FZO mediates fusion of mitochondria. However, mitochondrial morphology and ultrastructure in *fzl* mutants and *FZL-GFP* overexpressors were similar to those in WT (Fig. 8, which is published as supporting information on the PNAS web site). To further investigate whether FZL influences mitochondrial morphology, we crossed *fzl* mutants with WT plants expressing a mitochondrion-targeted form of GFP (29) and compared the morphology of the mitochondria in the F_2 progeny using fluorescence microscopy. We found no obvious differences between *fzl* and WT segregants with regard to mitochondrial size or morphology.

Discussion

We have shown that the plant protein FZL resembles FZO and its orthologs in sequence and domain arrangement. However, whereas

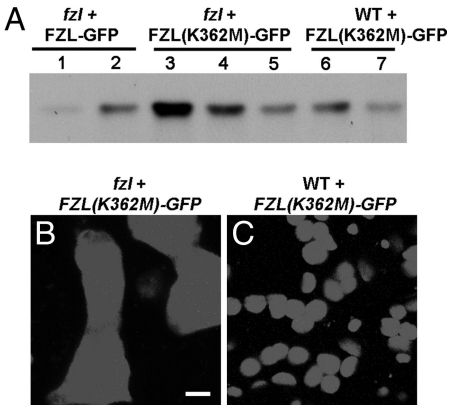

Fig. 5. Mutations in the GTPase domain abolish FZL-GFP function and punctate localization. (*A*) Immunoblot of leaf extracts from *fzl* (lanes 1–5) or WT plants (lanes 6 and 7) expressing FZL-GFP (lanes 1 and 2) or FZL(K362M)-GFP (lanes 4–7). Protein extracted from 2 mg of fresh weight was loaded in each lane. Lane 1, *fzl* partially complemented by a low level of FZL-GFP; lane 2, *fzl* fully complemented by FZL-GFP; lanes 3–5, *fzl* plants expressing FZL(K362M)-GFP at different levels; lanes 6 and 7, WT plants expressing FZL(K362M)-GFP. Samples in lanes 3 and 6 correspond to plants shown in *B* and *C*, respectively. (*B*) FZL(K362M)-GFP cannot complement the *fzl* phenotype. (*C*) FZL(K362M)-GFP in a WT plant. The punctate pattern of localization is not observed, as in Fig. 3 *K–N*. (Scale bar in *B*: 5 μm for *B* and *C*.)

FZO in fungi and animals is localized to outer mitochondrial membranes (1–3), FZL is localized inside chloroplasts. The most obvious defect associated with loss or gain of FZL function is a change in thylakoid organization. Grana in *fzl* mutants are stacked less evenly and are longer than in WT, and the unstacked stroma thylakoids comprise a lower proportion of the thylakoid network. Plants expressing FZL-GFP levels above those required to complement *fzl* also had longer grana stacks, but these had fewer lamellae than in WT or *fzl*. Like *fzl* mutants, these plants also had a reduced proportion of stroma thylakoids (Fig. 2*M*). It has been reported that chloroplasts maintain a constant proportion of grana and stroma thylakoids (30). Our results suggest a role for FZL in regulating or maintaining the distribution between the stacked and unstacked regions of the thylakoid network.

fzl mutants also exhibited heterogeneity in chloroplast size and number reminiscent of that observed in *Arabidopsis* plants deficient in the chloroplast division protein AtMinD1 (31, 32). We believe that this phenotype is an indirect effect of FZL depletion, perhaps arising from a change in membrane morphology or dynamics. We did not detect differences between *fzl* and WT plants with respect to total fatty acid or lipid composition (unpublished results). The distribution of membrane lipids could be altered, though, perhaps affecting association of AtMinD1 or other chloroplast division proteins with membranes and leading to division defects. However, overexpression of functional FZL-GFP did not cause chloroplast division defects.

FZO in fungi and animals is anchored in the outer mitochondrial membrane by two closely spaced TM helices that orient both N and C termini toward the cytosol. This topology allows FZO molecules on closely apposed mitochondria to interact via their coiled-coil domains to mediate outer-membrane fusion. The localization and protease protection assays on FZL, together with the similarity between FZL and FZO with regard to domain structure, strongly suggest that FZL is anchored in the inner envelope and thylakoid membranes by its two predicted TM domains with its N and C termini, including its predicted coiled-coil and GTPase domains, exposed to the stroma (Fig. 4*D*). By analogy to FZO (1, 2, 4, 11–14), this topological arrangement could allow interactions between FZL molecules on different membranes via their coiled-coil domains to stimulate a membrane fusion process that is important for determining thylakoid morphology. Additional studies will be required to fully dissect the topology of FZL and to test the hypothesis that FZL functions in the chloroplast as a membrane fusion protein.

The large number of GFP-labeled punctate structures in plants expressing relatively high levels of FZL-GFP (Fig. 3 *L* and *O*, lanes 7 and 8) may not reflect the authentic FZL distribution, because these plants probably accumulate the fusion protein at levels above those of FZL in WT. However, FZL-GFP was functional, and a few punctate structures were always observed at FZL-GFP levels sufficient to fully complement both the thylakoid morphology and chloroplast division defects in *fzl* (Fig. 3 *K* and *O*, lanes 5 and 6). Moreover, mutation of the conserved lysine in the FZL GTPase domain not only abolished the ability of the fusion protein to rescue the *fzl* mutant, but it also abolished its localization to punctate structures even though FZL(K362M)-GFP levels were comparable to those of FZL-GFP (Fig. 5). These results suggest that the puncta represent a physiologically relevant configuration of FZL and that their formation requires a functional GTPase domain.

Recent studies point to the importance of membrane remodeling as a crucial aspect of chloroplast morphogenesis and function. For example, vesicle trafficking from the inner envelope has been invoked as a key mechanism of thylakoid formation (19, 33, 34). Like FZL, two proteins implicated in chloroplast vesicle trafficking, VIPP1 and Thf1, affect thylakoid structure and are associated with thylakoid and envelope fractions (20, 21, 35). FZL could act in a related pathway, although the unique phenotype of *fzl* indicates that it has a distinct function. Collectively, these and other findings (27, 36), including observations that thylakoids directly contact the inner envelope (16), suggest that the inner envelope and thylakoid membranes form a dynamic continuum, consistent with the dual localization of FZL. Furthermore, a recent tomographic analysis has revealed foci of fusion between adjacent lamellae within a granum stack that are proposed as determinants of grana formation, stabilization, and interconnectivity (16). These results provide evidence for membrane fusion as an important factor in photosynthetic activity. Our findings of vesicle-like structures and abnormal grana and stroma thylakoid distribution in chloroplasts of *fzl* mutants, coupled with the similarity of FZL to the FZO class of membrane fusion proteins, implicates FZL in a membrane fusion process important in regulating the organization of the thylakoid network. Because FZL is the only FZO-like protein identifiable in plants and does not affect mitochondria, our work also raises the intriguing question of how mitochondrial morphology in plant cells is regulated.

Methods

Plant Material and Transformation. *Arabidopsis thaliana* ecotype Columbia (*Col-0*) was used as WT for all experiments. The *FZL* T-DNA insertion mutants Salk_033745 and Salk_009051 (23) were ordered from the *Arabidopsis* Biological Resource Center. The mutations are recessive, and homozygous *fzl* segregants were identified phenotypically. T-DNA insertion sites were verified by PCR and sequencing. Plant growth and transformation were performed as in ref. 37. Transgenic plants were selected by spraying with the herbicide Finale (AgrEvo Environmental Health, Montvale, NJ).

Microscopy. Leaf cell phenotypes were analyzed as described (37). GFP was detected in fresh leaf tissue as described in ref. 37 or by confocal laser scanning microscopy with a Zeiss PASCAL5.0 system (see *Supporting Methods*, which is published as supporting information on the PNAS web site).

For transmission electron microscopy of chloroplasts, 3-week-old leaf tissue was fixed as described in ref. 38. Postfixation, embedding, serial-sectioning of 70-nm-thin sections, and image capture were performed as in ref. 43. Images were processed with PHOTOSHOP imaging software (Adobe Systems, San Jose, CA).

Statistical Analysis of Thylakoid Morphology. The number and length of stroma and grana thylakoids falling on transect lines 1,050 nm on both sides of a line bisecting the long axis of a chloroplast were measured ($n = 15$ chloroplasts each for *WT*, *fzl*, and *FZL* complemented and overexpression lines: one chloroplast per cell, five chloroplasts per leaf, one leaf per plant, three plants). Stroma and grana thylakoids were defined as consisting of one or more than one lamella, respectively (Fig. 6). Number of lamellae per granum refers to the largest number of overlapping lamellae within the granum touching the transect (Fig. 6). Means were compared with Kruskal–Wallis one-way ANOVA on ranks by using SIGMASTAT software (version 2.03; SPSS, Chicago).

Sequence Analysis of FZL. Primers used for RT-PCR amplification of *FZL* cDNA were 5′-CACAGACGAAGGTATCTCACTCTC-3′ and 5′-TGTCAAGAAGGGAAAACCCGAC-3′. Amplified cDNAs were subcloned into Bluescript KS+ (Stratagene) before sequencing. The FZL amino acid sequence was deduced from the cDNA sequence. TARGETP (22) was used to predict the subcellular location of FZL. The TM domains of FZL were predicted by TMHMM (http://workbench.sdsc.edu) and TMPRED (www.ch.embnet.org/software/TMPRED_form.html). Coiled-coil domains were predicted with PAIRCOIL (39). The sequence alignment shown in Fig. 1*B* and phylogenetic analysis were performed by using the program CLUSTALW (40).

Test of the FZL Transit Peptide. pCAMBIA-1302-bar was generated by replacing the hygromycin-resistance marker in pCAMBIA-1302 (Cambia, Canberra, Australia) with a gene from pCAMBIA-3300 encoding resistance to the herbicide glufosinate. The coding sequence corresponding to amino acids 3–67 of FZL, which includes the predicted transit peptide, was inserted into pCAMBIA-1302-bar in frame with *GFP* to produce *35S-tpFZL-GFP* (see *Supporting Methods*). *35S-tpFZL-GFP*, or pCAMBIA-1302-bar as a negative control, was introduced into WT plants. GFP and chlorophyll were detected by fluorescence microscopy.

Complementation Analysis and FZL-GFP Localization. An *FZL* genomic fragment, including ≈740 bp of the 5′-flanking DNA, was amplified by PCR and ligated into pCAMBIA-1302-bar to produce *FZL-GFP* (see *Supporting Methods*). The construct was expressed in the Salk_009051 *fzl* mutant. T_1 plants were analyzed by microscopy and by immunoblotting (24) with monoclonal GFP antibodies (Molecular Probes, catalog no. A-11121) diluted 1:8,000.

Protease Protection Assays, Chloroplast Fractionation, and Immunoblotting. Chloroplast isolation, protease protection assays, and immunoblotting were performed as described (24, 41). Envelope and thylakoid fractions were prepared as in ref. 27 (see *Supporting Methods*). Crude proteins representing ≈4 μg of chlorophyll (41) in each lane were analyzed by SDS/PAGE, and immunoblotting. Tic110 and FtsZ1 antibodies were used as described (25, 42). GFP and LHCb antibodies were used at dilutions of 1:10,000 and 1:20,000, respectively.

Mutagenesis of *FZL*. *FZL(K362M)-GFP* was produced by PCR and subcloning into PCAMBIA-1302-bar (see *Supporting Methods*) and expressed in *fzl* (Salk_009051) and WT plants.

We thank Kathy Sault for help with TEM; Cecilia Chi-Ham for help with localization and assays; Bradley Olson and Yanfeng Zhang for experiments on recombinant proteins; Changcheng Xu, Bin Yu, and Hui Chen for performing fatty acid and lipid composition analyses; Maureen Hanson (Cornell University, Ithaca, NY) for seed stocks; Kenneth Cline (University of Florida, Gainesville) for LHCb antibodies; Kenneth Keegstra (Michigan State University, East Lansing) for Tic110 antibodies; and Kenneth Keegstra, John Froehlich, Jodi Nunnari, and Mary Fantacone for comments on the manuscript. This work was supported by grants from the National Science Foundation (to K.W.O.) and the Connaught Fund and Natural Sciences and Engineering Research Council of Canada (to T.L.S.).

1. Okamoto, K. & Shaw, J. M. (2005) *Annu. Rev. Genet.* **39,** 503–536.
2. Westermann, B. (2003) *Biochim. Biophys. Acta* **1641,** 195–202.
3. Meeusen, S. L. & Nunnari, J. (2005) *Curr. Opin. Cell Biol.* **17,** 389–394.
4. Meeusen, S., McCaffery, J. M. & Nunnari, J. (2004) *Science* **305,** 1747–1752.
5. Praefcke, G. J. & McMahon, H. T. (2004) *Nat. Rev. Mol. Cell Biol.* **5,** 133–147.
6. Hermann, G. J., Thatcher, J. W., Mills, J. P., Hales, K. G., Fuller, M. T., Nunnari, J. & Shaw, J. M. (1998) *J. Cell Biol.* **143,** 359–373.
7. Rapaport, D., Brunner, M., Neupert, W. & Westermann, B. (1998) *J. Biol. Chem.* **273,** 20150–20155.
8. Chen, H., Detmer, S. A., Ewald, A. J., Griffin, E. E., Fraser, S. E. & Chan, D. C. (2003) *J. Cell Biol.* **160,** 189–200.
9. Ishihara, N., Eura, Y. & Mihara, K. (2004) *J. Cell Sci.* **117,** 6535–6546.
10. Santel, A. & Fuller, M. T. (2001) *J. Cell Sci.* **114,** 867–874.
11. Rojo, M., Legros, F., Chateau, D. & Lombes, A. (2002) *J. Cell Sci.* **115,** 1663–1674.
12. Fritz, S., Rapaport, D., Klanner, E., Neupert, W. & Westermann, B. (2001) *J. Cell Biol.* **152,** 683–692.
13. Hales, K. G. & Fuller, M. T. (1997) *Cell* **90,** 121–129.
14. Koshiba, T., Detmer, S. A., Kaiser, J. T., Chen, H., McCaffery, J. M. & Chan, D. C. (2004) *Science* **305,** 858–862.
15. Trissl, H. W. & Wilhelm, C. (1993) *Trends Biochem. Sci.* **18,** 415–419.
16. Shimoni, E., Rav-Hon, O., Ohad, I., Brumfeld, V. & Reich, Z. (2005) *Plant Cell* **17,** 2580–2586.
17. Mustardy, L. & Garab, G. (2003) *Trends Plant Sci.* **8,** 117–122.
18. Morre, D. J., Sellden, G., Sundqvist, C. & Sandelius, A. S. (1991) *Plant Physiol.* **97,** 1558–1564.
19. Vothknecht, U. C. & Soll, J. (2005) *Gene* **354,** 99–100.
20. Wang, Q., Sullivan, R. W., Kight, A., Henry, R. L., Huang, J., Jones, A. M. & Korth, K. L. (2004) *Plant Physiol.* **136,** 3594–3604.
21. Kroll, D., Meierhoff, K., Bechtold, N., Kinoshita, M., Westphal, S., Vothknecht, U. C., Soll, J. & Westhoff, P. (2001) *Proc. Natl. Acad. Sci. USA* **98,** 4238–4242.
22. Emanuelsson, O., Nielsen, H., Brunak, S. & von Heijne, G. (2000) *J. Mol. Biol.* **300,** 1005–1016.
23. Alonso, J. M., Stepanova, A. N., Leisse, T. J., Kim, C. J., Chen, H., Shinn, P., Stevenson, D. K., Zimmerman, J., Barajas, P., Cheuk, R., *et al*. (2003) *Science* **301,** 653–657.
24. McAndrew, R. S., Froehlich, J. E., Vitha, S., Stokes, K. D. & Osteryoung, K. W. (2001) *Plant Physiol.* **127,** 1656–1666.
25. Jackson, D. T., Froehlich, J. E. & Keegstra, K. (1998) *J. Biol. Chem.* **273,** 16583–16588.
26. Vitha, S., Froehlich, J. E., Koksharova, O., Pyke, K. A., van Erp, H. & Osteryoung, K. W. (2003) *Plant Cell* **15,** 1918–1933.
27. Block, M. A., Tewari, A. K., Albrieux, C., Marechal, E. & Joyard, J. (2002) *Eur. J. Biochem.* **269,** 240–248.
28. Saraste, M., Sibbald, P. R. & Wittinghofer, A. (1990) *Trends Biochem. Sci.* **15,** 430–434.
29. Kohler, S., Delwiche, C. F., Denny, P. W., Tilney, L. G., Webster, P., Wilson, R. J., Palmer, J. D. & Roos, D. S. (1997) *Science* **275,** 1485–1489.
30. Albertsson, P.-A. & Andreasson, E. (2004) *Physiologia Plant* **121,** 334–342.
31. Colletti, K. S., Tattersall, E. A., Pyke, K. A., Froelich, J. E., Stokes, K. D. & Osteryoung, K. W. (2000) *Curr. Biol.* **10,** 507–516.
32. Fujiwara, M. T., Nakamura, A., Itoh, R., Shimada, Y., Yoshida, S. & Moller, S. G. (2004) *J. Cell Sci.* **117,** 2399–2410.
33. Vothknecht, U. C. & Westhoff, P. (2001) *Biochim. Biophys. Acta* **1541,** 91–101.
34. Andersson, M. X. & Sandelius, A. S. (2004) *BMC Genomics* **5,** 40.
35. Li, H. M., Kaneko, Y. & Keegstra, K. (1994) *Plant Mol. Biol.* **25,** 619–632.
36. Tottey, S., Block, M. A., Allen, M., Westergren, T., Albrieux, C., Scheller, H. V., Merchant, S. & Jensen, P. E. (2003) *Proc. Natl. Acad. Sci. USA* **100,** 16119–16124.
37. Gao, H., Kadirjan-Kalbach, D., Froehlich, J. E. & Osteryoung, K. W. (2003) *Proc. Natl. Acad. Sci. USA* **100,** 4328–4333.
38. Hall, J. L. & Hawes, D. (1991) *Electron Microscopy of Plant Cells* (Academic, London).
39. Berger, B., Wilson, D. B., Wolf, E., Tonchev, T., Milla, M. & Kim, P. S. (1995) *Proc. Natl. Acad. Sci. USA* **92,** 8259–8263.
40. Thompson, J. D., Higgins, D. G. & Gibson, T. J. (1994) *Nucleic Acids Res.* **22,** 4673–4680.
41. Bruce, B. D., Perry, S., Froehlich, J. & Keegstra, K. (1994) in *Plant Molecular Biology Manual J1*, eds. Gelvin, S. B. & Schilperoort, R. B. (Kluwer, Boston), pp. 1–15.
42. Stokes, K. D., McAndrew, R. S., Figueroa, R., Vitha, S. & Osteryoung, K. W. (2000) *Plant Physiol.* **124,** 1668–1677.
43. Hristova, K., Lam, M., Feild, T. & Sage, T. L. (2005) *Ann. Bot. (London)* **96,** 779–791.